Hyperfine Interactions 38 (1987) 435–470

AN OPTICAL PUMPING PRIMER

W. HAPPER and W.A. VAN WIJNGAARDEN

Princeton University, Princeton, N.J. 08544, U.S.A.

This pedagogical paper introduces the basic ideas of optical pumping. Some of the various optical pumping mechanisms are discussed, and illustrated by diagrams showing the experimental apparatus. The density matrix formalism is introduced and used to quantitatively examine the effects of optical pumping. Next some of the various spin relaxation mechanisms such as collisions and spin exchange between electrons and nuclei, are discussed. A good knowledge of elementary quantum mechanics is needed to follow the article.

1. Introduction

The basic idea of optical pumping [1] for which A. Kastler [2] received the Nobel Price in 1966, is that the photons of a beam of light can transfer order to atoms or molecules by resonant scattering. Experiments in optical pumping are often very simple and inexpensive, but they can yield amazingly precise spectroscopic information and also very important information about interatomic forces. In these pedagogical notes we shall try to introduce some of the most important ideas of optical pumping. A good knowledge of elementary quantum mechanics is needed to follow the subsequent discussion. We have intentionally left as exercises the completion of a number of steps in the arguments.

The basic parts of an optical pumping experiment are a lamp or a laser to provide pumping light, a dilute gas of atoms which absorbs and scatters the photons and which becomes spin polarized as a result, and a means to detect the degree of atomic polarization. This can be as simple as an optical detector to monitor changes in the amount of transmitted or scattered light. The pumped atoms may be mixed with more abundant molecules or atoms of a buffer gas. An inert buffer gas like helium or neon is often used to hinder the diffusion of spin polarized atoms to the walls of the container. Molecular buffer gases like N_2 or H_2 are often used to quench optically excited atoms, i.e. to eliminate reradiated resonance light, which can be multiply scattered and which can cause spin depolarization. Other paramagnetic atoms in the same cell can become spin polarized by *spin exchange* collisions with the optically pumped atoms.

2. Anisotropic excitation

The simplest type of optical pumping and perhaps the most important in terms of spectroscopic results is *anisotropic optical excitation*. An example is shown in fig. 1. The quantization axis z is chosen to point along the polarization direction of the linearly polarized resonance light. In practice, it is often convenient to apply a small magnetic field along the z direction to prevent stray magnetic fields pointing perpendicular to the quantization axis from depolarizing the atoms. The resonant light excites the atoms from the nondegenerate ground state with angular momentum quantum number $J=0$ to the $m=0$ Zeeman sublevel of an excited state with angular momentum $J=1$. The excited atom is spin polarized since the magnetic sublevels are not equally populated. A simple way to detect the spin polarization is to observe the characteristic dipole radiation pattern of the fluorescent light. No photons are emitted parallel or antiparallel to the direction of the magnetic field, but π polarized photons are emitted in all directions perpendicular to the magnetic field.

Anisotropic excitation creates highly polarized atoms. It is the first step in many important spectroscopic methods like optical double resonance [3] or level crossing [4] spectroscopy. The atomic spin polarization is nearly independent of the intensity of the exciting light, but not many atoms can be accumulated because the excited atoms decay so quickly by fluorescing or by quenching

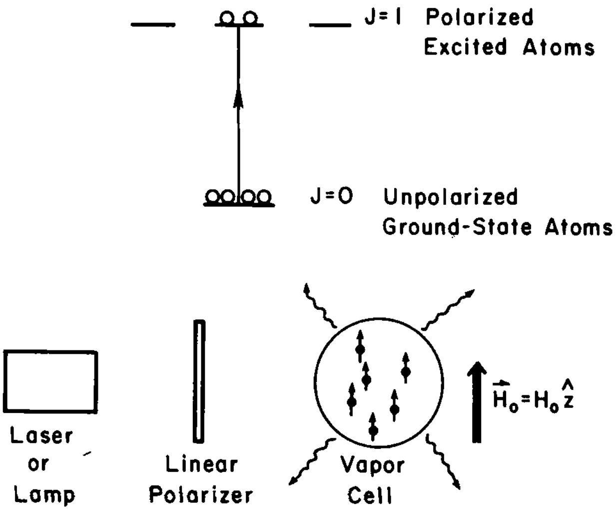

Fig. 1. Anisotropic optical excitation. Linearly polarized light from a lamp or laser excites only the $m=0$ sublevel of the excited state. The quantization axis z is specified by the polarization direction of the pump light. In practice, a small magnetic field H_0 is applied along the z axis to reduce the depolarization of the atom by stray magnetic fields pointing perpendicular to H_0.

collisions with molecular gases like N_2 or H_2 which carry off the excitation energy in vibrational and rotational degrees of freedom.

3. Depopulation pumping

A second optical pumping method, *depopulation pumping*, can be used to generate much large numbers of spin polarized atoms in their ground states or metastable states. Depopulation refers to the selective excitation of one or more particular sublevels and hence a reduction of their population. Two examples are shown in fig. 2. In case a, circularly polarized light is used to pump atoms from the magnetic sublevel with $m = 1/2$ to the $m = 1/2$ state of the upper level which

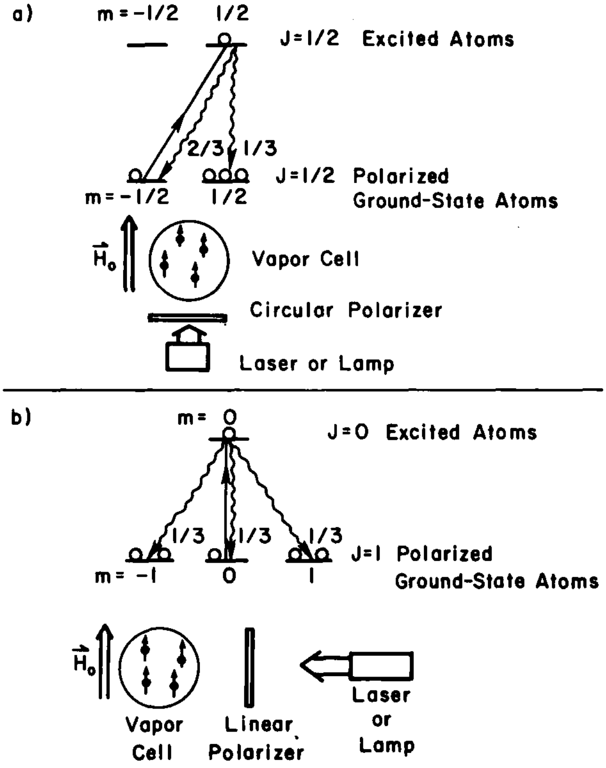

Fig. 2. Depopulation pumping. Polarized light is used to deplete the population of a ground state sublevel. In part (a), circularly polarized light excites the ground state $m = -1/2$ sublevel to the excited state $m = 1/2$ sublevel. The excited atoms will spontaneously decay to either ground state sublevels with the indicated branching ratios (repopulation pumping). After sufficient time, all the atoms will be polarized in the $m = 1/2$ ground state sublevel. In part (b), linearly polarized light is used to depopulate the $m = 0$ ground state sublevel leaving the atoms polarized in the $m = \pm 1$ sublevels of the ground state.

then spontaneously decays, repopulating either of the spin sublevels of the ground state with the branching ratios indicated in the figure. After a few photons have been scattered by the atom, all of the atoms will have been pumped to the 1/2 sublevel and no further scattering will occur. In case b, linearly polarized light excites atoms from the magnetic sublevel with $m = 0$ into an excited state of angular momentum $J = 0$. The excited atom decays with equal probability to any of the three ground-state sublevels. After a few photons have been scattered by the atom, half of the atoms will be in the sublevel with $m = 1$ and half will be in the sublevel with $m = -1$ and none in the sublevel with $m = 0$. Note that in both of these examples the spin sublevels with the largest absorption cross sections are most strongly depopulated by the optical pumping. In depopulation pumping it does not matter much whether the excited state decays by spontaneous emission of radiation or whether the atom is deexcited by some non-radiative quenching collision with a molecule of the buffer gas. Depopulation pumping can work well at buffer gas pressures of atmospheres or more, provided the buffer gas does not cause transitions between the spin sublevels of the ground state.

4. Repopulation pumping

Repopulation pumping, refers to the transfer of polarization of an excited state to a lower state. For example in fig. 2a, spin polarized excited atoms populate a lower state by spontaneous radiative decay. The selection rules are such that some of the spin polarization of the excited state is transferred to the ground state. In the case shown in fig. 2a, the polarization transferred to the ground state is $-1/3$ times as large as the spin polarization of the excited atom.

EXERCISE 1

Verify that the polarization transfer factor is $-1/3$ for the example shown in fig. 1.

Repopulation pumping will not work if the excited atom loses its polarization by collisions with buffer gas atoms before it has a chance to spontaneously decay. Therefore, depopulation pumping works best at very low buffer gas pressures where collisions are too infrequent to depolarize the excited atoms.

We note that some spontaneous process is needed to carry away the entropy of atoms as they become spin polarized by optical pumping. This is similar to the situation in nuclear magnetic resonance where lattice phonons are used to carry off nuclear spin entropy as the nuclei become spin polarized by microwave pumping in the ENDOR technique [5]. In optical pumping, fluorescent photons or quenching collisions are used to carry off the entropy.

5. Optical pumping rate equations

The main features of optical pumping can be understood with the aid of rate equations, which describe optically induced transfers of population between spin sublevels of an atom. Consider, for example, the case of an atom with a spin-1/2 ground state and a spin-1/2 excited state, pumped by circularly polarized light. The situation is sketched in fig. 2a. The σ_+ light can only excite atoms in the sublevel with azimuthal quantum number $m = -1/2$. The rates of change of the number densities $\rho(1/2)$ and $\rho(-1/2)$ of atoms in the sublevels with $m = 1/2$ and $m = -1/2$ respectively are therefore given by

$$\frac{\mathrm{d}}{\mathrm{d}t}\rho(-1/2) = -2R\rho(-1/2) + (\tfrac{2}{3})2R\rho(-1/2) \tag{1}$$

$$\frac{\mathrm{d}}{\mathrm{d}t}\rho(1/2) = 0 + (\tfrac{1}{3})2R\rho(-1/2). \tag{2}$$

In each equation the first term describes depopulation pumping and the second term describes repopulation pumping. The factors 2/3 and 1/3 are the branching ratios for spontaneous decay of an atom in the upper state sublevel with azimuthal quantum number 1/2 to the ground-state sublevels with $m = 1/2$ and $m = -1/2$ respectively. Note that we obtain a simpler pair of equations for the sum and difference of the ground-state sublevel populations, which we write as

$$N_\mathrm{g} = \rho(1/2) + \rho(-1/2) \tag{3}$$

$$(S_z) = \frac{1}{2N_\mathrm{g}}[\rho(1/2) - \rho(-1/2)]. \tag{4}$$

Equations (1) and (2) imply that

$$\frac{\mathrm{d}N_\mathrm{g}}{\mathrm{d}t} = 0, \tag{5}$$

Thus we conclude that N_g is a constant, which is consistent with our tacit assumption that the optical pumping rates are so slow that the atoms spend most of their time in the ground state. Henceforth, we shall assume that

$$N_\mathrm{g} = 1.$$

We may now regard $\rho(1/2)$ and $\rho(-1/2)$ as the occupation probabilities of the sublevels with azimuthal quantum numbers $m = 1/2$ and $m = -1/2$ respectively. The corresponding equation for (S_z) is

$$\begin{aligned}\frac{\mathrm{d}(S_z)}{\mathrm{d}t} &= \tfrac{2}{3}R\rho(-1/2)\\ &= \tfrac{1}{3}R(1 - 2\langle S_z\rangle). \end{aligned}\tag{7}$$

We can readily solve (6), with the initial condition $\langle S_z \rangle = 0$ at $t = 0$, to find

$$\langle S_z \rangle = \tfrac{1}{2}(1 - \mathrm{e}^{-2Rt/3}). \tag{8}$$

That is, the spin polarization builds up from 0 to within 1/e of its maximum possible value in a time $3/(2R)$.

EXERCISE 2
Derive (8) from (7).

We can also calculate the number of photons needed to polarize the atom with this simple model. According to (1) the rate of scattering of photons is

$$\begin{aligned}\frac{\mathrm{d}n}{\mathrm{d}t} &= 2R\rho(-1/2)\\ &= R[1 - 2\langle S_z \rangle]\\ &= R\ \mathrm{e}^{-2Rt/3}.\end{aligned} \tag{9}$$

The total number of scattered photons is then

$$n = \int_0^\infty \frac{\mathrm{d}n}{\mathrm{d}t}\mathrm{d}t = 3/2. \tag{10}$$

EXERCISE 3
Derive (10 from (9).

We see that one and a half photons, on the average, are required to fully polarize the initially unpolarized atom. Real optical pumping situations are somewhat more complicated than the simple model discussed above, but it is always true that in the absence of spin relaxation mechanisms, an atom will reach its equilibrium polarization after scattering a small number of photons. The model discussed above is a particularly favorable situation since in equilibrium all atoms are in the $+1/2$ sublevel. Hence no further scattering of photons can occur. In other situations the equilibrium polarization can be less than 100%, and scattering of photons still occurs.

It is often convenient to optically pump an atom in the presence of a buffer gas at such high pressures that the excited atoms are completely depolarized before they decay. Then there will be no repopulation pumping and the spin polarization will build up solely because of depopulation pumping. Let us see what happens in the situation discussed above if there is no repopulation pumping. The optical pumping rate equations (1) and (2) become

$$\frac{\mathrm{d}}{\mathrm{d}t}\rho(-1/2) = -2R\rho(-1/2) + (\tfrac{1}{2})2R\rho(-1/2) \tag{11}$$

$$\frac{\mathrm{d}}{\mathrm{d}t}\rho(1/2) = 0 + (\tfrac{1}{2})2R\rho(-1/2) \tag{12}$$

and the evolution of the spin polarization would be described by

$$\frac{\mathrm{d}}{\mathrm{d}t}\langle S_z\rangle = = \tfrac{1}{2}R(1 - 2\langle S_z\rangle). \tag{13}$$

The solution of (13) is

$$\langle S_z\rangle = \tfrac{1}{2}(1 - \mathrm{e}^{-Rt}). \tag{14}$$

Following through the calculation of the average number of photons needed to fully polarize an initially unpolarized atom, we find in analogy to (10)

$$n = 1.$$

That is, only one photon instead of 1.5 photons is needed to polarize each initially unpolarized atom. For the simple case discussed above, collisional depolarization of the excited state or "mixing" in the excited state improves the efficiency of optical pumping. The depopulation pumping tends to polarize the ground state in the same direction as the photon spin, while the repopulation pumping tends to polarize the ground state in the opposite direction from the photon spin. However, the depopulation pumping dominates and the equilibrium atomic polarization is always in the same direction as the photon spin, whether or not mixing occurs in the excited state.

The relative importance of depopulation and repopulation pumping depends on the particular state being pumped. For example, if circularly polarized D_2 light is used to optically pump an alkali atom, as sketched in fig. 3, the $m = 1/2$ ground state sublevel is 3 times more likely to be excited than the $m = -1/2$ sublevel. Hence depopulation pumping tends to polarize the ground state of the atom in the direction opposite to that of the photon spin. Next, the excited state radiatively decays, repopulating the ground state. Repopulation pumping tends to polarize the ground state in the same direction as the photon spin since the $m = 1/2$ excited state sublevel can decay to either of the $m = \pm 1/2$ ground state

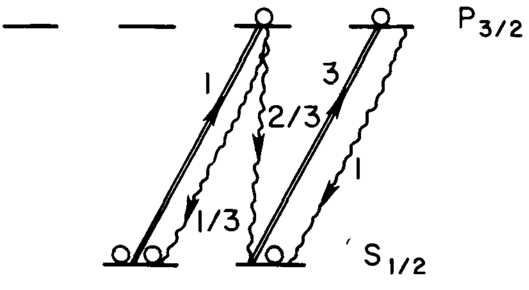

Fig. 3. Effects of depopulation and repopulation pumping. Depopulation pumping using circularly polarized D_2 light polarizes the ground state in the direction opposite to the photon spin. Repopulation pumping tends to polarize the atomic ground state parallel to the pump photon spin. Here we have neglected possible depolarization of the excited state due to collisions.

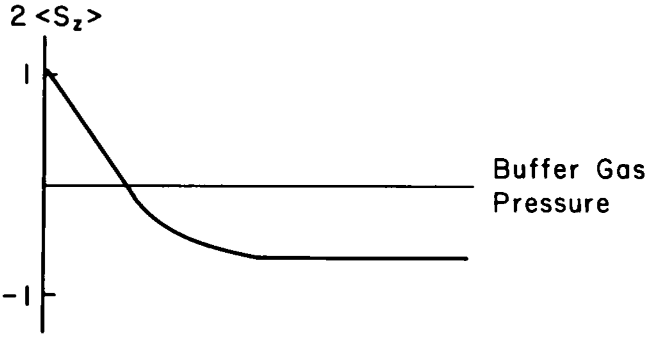

Fig. 4. Effect of buffer gas pressure on ground state polarization. When pumping an alkali atom with circularly polarized D_2 light, depopulation pumping polarizes the ground state in the direction opposite to the photon spin, while repopulation pumping, in the absence of collisional depolarization of the excited state, tends to polarize the ground state parallel to the pump photon spin (see fig. 3). At low buffer gas pressure, repopulation pumping predominates while at high pressures it becomes negligible and the ground state polarization is negative.

sublevels while the $m = 3/2$ excited state sublevel only decays to the $m = 1/2$ sublevel. In the absence of collisional depolarization of the excited state, the ground state will be polarized parallel to the photon spin due to repopulation pumping. At high buffer gas pressures, collisions depolarize the excited state and repopulation pumping is greatly reduced. The atoms are then polarized in a direction antiparallel to the photon spin due to depopulation pumping. Thus, the equilibrium ground-state spin polarization depends on the buffer gas pressure and equals zero at a pressure of a few Torr where the effects of depopulation and repopulation pumping are equal and opposite, as indicated in fig. 4. Franz [6] has estimated collisional mixing cross sections for the ${}^2P_{3/2}$ states of alkali atoms by using the zero polarization pressures for the phenomenon sketched in fig. 4.

6. The density matrix

In the simple examples of a spin-1/2 atom discussed above we have been making use of the occupation probabilities $\rho(+1/2)$ of the ground state sublevels with azimuthal quantum numbers $m = \pm 1/2$. These occupation probabilities are in fact the diagonal elements of the atomic density operator ρ. Suppose that we have a collection of N atoms, each with its own wavefunction $|\psi_i\rangle$ $i = 1, 2, 3 \ldots N$. Then the mean value of some atomic observable, say the electron spin, is

$$\begin{aligned}\langle \boldsymbol{S} \rangle &= \frac{1}{N} \sum_{i=1}^{N} \langle \psi_i | \boldsymbol{S} | \psi_i \rangle \\ &= \mathrm{Tr}[\boldsymbol{S}\rho],\end{aligned}$$

where the density operator is

$$\rho = \frac{1}{N}\sum |\psi_i\rangle\langle\psi_i|. \tag{17}$$

For a spin-1/2 atom the density operator has four components

$$\begin{aligned}\rho = {}& |1/2\rangle\langle 1/2|\rho|1/2\rangle\langle 1/2| + |1/2\rangle\langle 1/2|\rho|-1/2\rangle\langle -1/2| \\ & + |-1/2\rangle\langle -1/2|\rho|1/2\rangle\langle 1/2| + |-1/2\rangle\langle -1/2|\rho|-1/2\rangle\langle -1/2|.\end{aligned} \tag{18}$$

The occupation probabilities $\rho(\pm 1/2)$ of the preceding discussion are obviously abbreviations of $\langle \pm 1/2|\rho|\pm 1/2\rangle$. To increase the physical significance of the density matrix we introduce a complete set of operators

$$S_z = \tfrac{1}{2}[\,|1/2\rangle\langle 1/2| - |-1/2\rangle\langle -1/2|\,] \tag{19}$$

$$S_+ = S_z + \mathrm{i}S_y = |1/2\rangle\langle -1/2| \tag{20}$$

$$S_- = S_x - \mathrm{i}S_y = |-1/2\rangle\langle 1/2| \tag{21}$$

$$1 = |1/2\rangle\langle 1/2| + |-1/2\rangle\langle -1/2|. \tag{22}$$

Eliminating the operators $|1/2\rangle\langle 1/2|$, $|1/2\rangle\langle -1/2|$ etc. from (18) with the aid of (19) – (22) we find that we may write ρ in the convenient form

$$\rho = \tfrac{1}{2} + 2\langle \boldsymbol{S}\rangle \cdot \boldsymbol{S}, \tag{23}$$

where $\langle S_z\rangle$ was given by (4) and

$$\langle S_+\rangle = \mathrm{Tr}(S_+\rho) = \langle -1/2|\rho|1/2\rangle \tag{24}$$

$$\langle S_-\rangle = \mathrm{Tr}(S_-\rho) = \langle 1/2|\rho|-1/2\rangle. \tag{25}$$

Expansions of the density operator which are similar to (23) can be written for higher-spin atoms and for atoms with several interacting spins, e.g. electronic and nuclear spins.

EXERCISE 4

For a spin-1 atom show that a diagonal density operator can always be written as

$$\rho = \tfrac{1}{3} + \tfrac{1}{2}\langle S_z\rangle S_z + \tfrac{1}{6}\langle 3S_z^2 - 2\rangle(3S_z^2 - 2).$$

7. Optical monitoring of spin polarization

Under many experimental conditions the rate of photon scattering (9) is used as the "signal" which gives information about the degree of spin polarization of

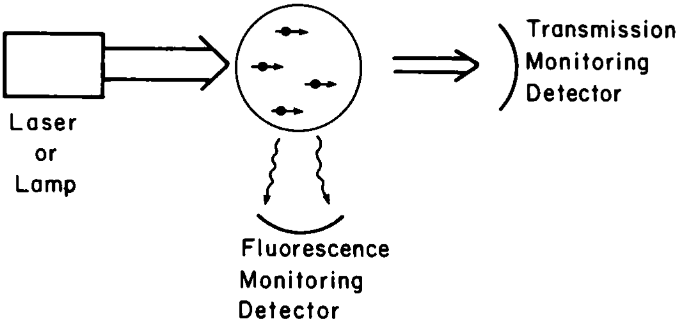

Fig. 5. Detection of spin polarization. The atomic spin polarization can be monitored by measuring either the attenuation of pump light after it has passed through the cell or the amount of fluorescence light scattered by the atoms.

the atoms. In the simple case discussed above, the signal is a superposition of a constant term R, the mean photon scattering rate, and a polarization-dependent term, $-2R\langle S_z\rangle$. There are two ways to measure the photon scattering rate, which are illustrated in fig. 5. One can observe the attenuation of the pumping light after it has passed through the cell, a method called *transmission monitoring*, or one can measure the amount of fluorescence light scattered by the optically pumped atoms, a method known as *fluorescence monitoring*. Both methods usually involve some kind of averaging over the variations of light intensity and spin polarization within the cell. The interpretation of the data is easiest when the cells are optically thin and scatter only a small fraction of the light, but the signal to noise ratio is best when the cell attenuates about half of the pumping light.

The fluorescence monitoring detector should be as sensitive as possible, preferably a photomultiplier tube since the fluorescence signals may be weakened by quenching gases and are distributed over 4π steradians of solid angle. The transmission monitoring signal is ordinarily much too intense to require or permit the use of a photomultiplier tube, and a simple vacuum photocell or a solid state photoconductive detector is usually adequate. If a quenching gas like nitrogen is used, which is sometimes essential to eliminate radiation trapping for high-density atomic vapors, there will be negligible fluorescence, and transmission monitoring is the only choice for optical detection of spin polarization.

From a formal point of view, both fluorescence monitoring and transmission monitoring can be described by noting that the photon scattering cross section can be regarded as the expectation value of a spin-dependent cross section operator, i.e.

$$\langle \rho \rangle = \mathrm{Tr}(\rho\sigma). \tag{26}$$

In the simple case illustrated in fig. 1a of a spin-1/2 ground state atom, the cross section operator can be written as

$$\sigma = \sigma_0[1 - 2\boldsymbol{s}\cdot\boldsymbol{S}], \tag{27}$$

where $\boldsymbol{s}$ is the mean spin of the photons and σ_0 is the cross section for the scattering of light by unpolarized atoms. The cross section σ_0 is a function of frequency which is strongly peaked at the resonance frequency of the transition. We see from (23) that the mean pumping rate R of (1) must be related to the spectral intensity $I(\nu)$ (erg cm^{-2} sec^{-1} Hz^{-1}) and the cross section $\sigma_0(\nu)$ by

$$R = \int \frac{\sigma_0(\nu)I(\nu)}{h\nu}\,\mathrm{d}\nu. \tag{28}$$

8. Slow spin relaxation in binary collisions

We turn now to consider the effect of spin relaxation. Optically pumped atoms are often subject to various collisional processes. For example, the atoms can collide with the container walls or with other gaseous atoms or molecules in the cell. It is a remarkable fact that under the proper conditions an atom which has been spin polarized by optical pumping can undergo a huge number of momentum-changing collisions with no loss of spin polarization. [1] For example, a sodium atom can undergo some 10^9 collisions with helium buffer gas atoms before its electron spin is flipped. A ^{3}He atom can undergo at least 10^8 collisions with the glass walls of a cell before losing its nuclear spin polarization.

When a spin polarized atom approaches another atom, for example, a noble gas atom like He or Ar, the pair can be thought of as a temporary diatomic molecule. For example, we have sketched in fig. 6 the adiabatic energy levels E_Ω of an alkali atom as a function of the internuclear distance between the alkali atom and the noble gas atom. Noble gases or diamagnetic molecular gases like N_2 or H_2 are often used as buffer gases for optically pumped atoms.

As we shall explain below, one can expect to find very slow spin relaxation whenever the potential curve which represents the interaction between the buffer gas atom and the spin-polarized atom, does not split into several curves corresponding to different spin orientations when the perturber comes close. Thus, the ground-state alkali atom illustrated in fig. 6 can be expected to relax very slowly, since the lowest molecular potential curve does not split. However, an alkali atom in the $^2P_{3/2}$ excited state should depolarize very readily. Both phenomena are observed experimentally.

The electronic Hamiltonian of a pair of atoms like those of fig. 6 can be written as

$$H = H_0(R) + \Delta H, \tag{29}$$

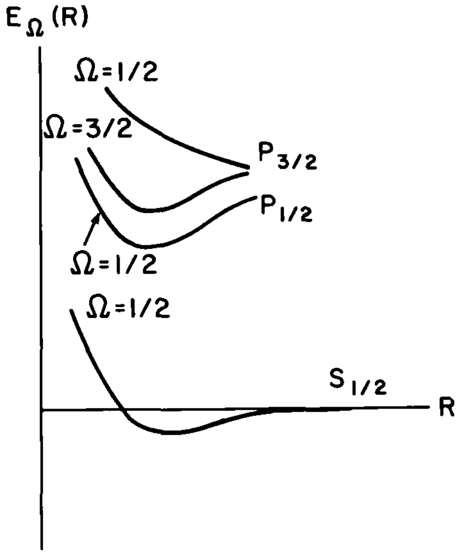

Fig. 6. Perturbation of the energy levels of an alkali atom by a nearby noble gas atom. R is the internuclear distance separating the alkali and noble gas atom. Ω is the absolute value of the azimuthal quantum number of the electronic wavefunction about the internuclear axis.

where H_0 is the electronic Hamiltonian for the atoms at rest at the equilibrium internuclear separation R. We can write

$$H_0 = T_e + V_{\mathrm{Coul}} + \overline{V}_{\mathrm{SO}}, \tag{30}$$

where T_e is the kinetic energy operator of the electrons, V_{Coul} is the Coulomb energy of attraction of the electrons to the atomic nuclei and the energy of repulsion between the electrons. Finally, $\overline{V}_{\mathrm{SO}}$ is the first-order part of the spin-orbit interaction between the moving electron spins and the electric fields within the molecule. The term ΔH of (29) denotes the higher-order effects of spin-orbit interactions, which are associated with the excitation of electronic states or the motion of the nuclei. Also included in ΔH are the spin-spin interactions and other small terms which are described in more detail in most textbooks on molecular spectroscopy.

As indicated in fig. 6, the valence electron of the alkali atom will have its wavefunctions and energies strongly perturbed as soon as the unperturbed wavefunction overlaps the noble gas atom. The main cause of the perturbation is the electrostatic potential experienced by the alkali valence electron in the core of the noble gas atom. There is a substantially smaller contribution from the spin-orbit interaction. Since both the electrostatic and the spin-orbit potentials are invariant with respect to rotations about the internuclear axis, we can label the eigenstates of the alkali-noble-gas pair with an azimuthal quantum number m, i.e.

$$J_\zeta \,|m\rangle = m\,|m\rangle, \tag{31}$$

where J_ζ is the projection of the total electronic angular momentum operator on the internuclear axis ζ. The electrostatic and spin-orbit interactions are invariant to the time-reversal operator T, that is, $H_0T = TH_0$, and since $T\,|m\rangle \propto |-m\rangle$ we can conclude from elementary quantum mechanics that the quantum states $|m\rangle$ and $|-m\rangle$ are degenerate in energy. In other words, setting

$$\Omega = |m| \tag{32}$$

we have

$$E_\Omega = E_{-\Omega}. \tag{33}$$

Of course, this is the well known theorem of Kramers. If the total electronic angular momentum of the spin polarized atom is J, the perturber will split the atomic ground state into $J + \frac{1}{2}$ Kramer doublets if J is a half integer or into J doublets, and a single sublevel with $m = 0$, if J is even.

Let the atom be described before the collision by the initial wavefunction

$$|\psi_\mathrm{i}\rangle = \sum_{m=-J}^{J} |m\rangle\langle m|\psi_\mathrm{i}\rangle. \tag{34}$$

After the collision the final wavefunction will be

$$|\psi_\mathrm{f}\rangle = \sum_{m=-J}^{J} |m\rangle\langle m|\psi_\mathrm{i}\rangle\, \mathrm{e}^{-\mathrm{i}\phi(m)}, \tag{35}$$

where the phase shift is

$$\phi(m) = \int_{-\infty}^{\infty} \frac{E(m,\,t)}{\hbar}\,\mathrm{d}t. \tag{36}$$

Here $E(m,\,t)$ is the adiabatic electronic energy as a function of time t, and m is the azimuthal quantum number of (31). If the interaction energies are identical for all components of the wavefunction, i.e.

$$E(m) = E_0 \text{ where } -J \le m \le J \tag{37}$$

then we can factor out a common phase factor and write

$$|\psi_\mathrm{f}\rangle = \mathrm{e}^{-\mathrm{i}\phi_0}\,|\psi_\mathrm{i}\rangle. \tag{38}$$

But a common phase factor has no influence on the expectation value of spin observables, for example, if (38) is true then

$$\langle\psi_\mathrm{f}|\boldsymbol{S}|\psi_\mathrm{f}\rangle = \langle\psi_\mathrm{i}|\boldsymbol{S}|\psi_\mathrm{i}\rangle. \tag{39}$$

Hence, we conclude that atoms which can be described as linear superpositions of states which remain degenerate during the course of a collision should experience no spin relaxation at all. This is the case, at least to lowest order, for atoms with total angular momentum $J = 1/2$, like alkali atoms in their $^2S_{1/2}$ ground states or in their $^2P_{1/2}$ excited states of thallium atoms in their $^2P_{1/2}$ ground states. S-state atoms (i.e. atoms for which the orbital angular momentum is zero.) with total electronic spin $S = J > \frac{1}{2}$ also relax very slowly in buffer gases because the splitting of the Kramer doublets is very small and is due to the weak spin-spin and spin-orbit interactions instead of the much larger electrostatic interactions which split the Kramers doublets for non-S-state atoms. Thus, nitrogen and phosphorus atoms which have $^4S_{3/2}$ ground states corresponding to half-filled P shells, relax very slowly in buffer gases [7].

If the atom has no electronic angular momentum at all, i.e. $J = 0$ in the ground state, the atom may still carry nuclear spin polarization. Important examples are ^{199}Hg, ^{201}Hg, ^{3}He, ^{129}Xe, ^{131}Xe etc. The collisional relaxation of these diamagnetic atoms is exceptionally slow, and the relaxation times can be minutes, hours or even days in the case of ^{3}He.

9. Spin rotation interaction

The preceding discussion shows why alkali atoms with their $^2S_{1/2}$ ground states should exhibit very slow spin relaxation due to collisions with buffer gas atoms. It is indeed true that polarized alkali atoms relax very slowly, but some relaxation is observed. This slow residual spin relaxation was the subject of much confusion in the early optical pumping literature. Bernheim [8] first pointed out that the spin-rotation interaction

$$V_{sr} = \gamma \boldsymbol{S} \cdot \boldsymbol{N} \tag{40}$$

between the electron spin $\boldsymbol{S}$ of the alkali atom and the rotational angular momentum $\boldsymbol{N}$ of the alkali-noble-gas pair would lead to spin relaxation. Bernheim made some rough theoretical estimates of the magnitude of the spin-rotation coupling constant γ which were in qualitative agreement with experiment. Soon thereafter, R. Herman [9] made more elaborate theoretical estimates of γ which seemed to be in fair agreement with the experimental data available at that time. A very simple theory of γ which is in better agreement with the most recent experimental findings has been reported by Wu et al. [10]. We shall not dwell on the microscopic theory of γ here, but will show how the spin-rotation interaction causes spin relaxation of alkali atoms.

Consider a binary collision between an alkali atom and a noble gas atom. The alkali atom wavefunction ψ_f after the collision is related to the initial wavefunction ψ_i before the collision by the solution to Schroedinger's equation

$$\begin{aligned} |\psi_\mathrm{f}\rangle &= \left(\exp\frac{-\mathrm{i}}{\hbar}\int V_\mathrm{sr}\,\mathrm{d}t\right)\psi_\mathrm{i}\rangle \\ &= (\exp - \mathrm{i}\boldsymbol{\phi}\cdot\boldsymbol{S})\,|\psi_\mathrm{i}\rangle, \end{aligned} \tag{41}$$

where the electron spin rotation angle is

$$\boldsymbol{\phi} = \frac{\boldsymbol{N}}{\hbar}\int_{-\infty}^{\infty}\gamma\,\mathrm{d}t \tag{42}$$

and we have approximated the rotational angular momentum with the constant classical vector $\boldsymbol{N}$. As to order of magnitude, experiments show that $\gamma/h \leq 10^6$ Hz. The duration of a binary collision is $\tau \approx 10^{-12}$ sec (Bohr radius/speed of sound), and $N \approx 100$ so the rotation angle ϕ is on the order of only 10^{-4} radians. We can rewrite (41) in terms of the density matrix as

$$\rho_\mathrm{f} = \langle \mathrm{e}^{-\mathrm{i}\boldsymbol{\phi}\cdot\boldsymbol{S}}\rho_\mathrm{i}\,\mathrm{e}^{-\mathrm{i}\boldsymbol{\phi}\cdot\boldsymbol{S}}\rangle, \tag{43}$$

where the angle brackets denote an average over all possible collisional rotation angles $\boldsymbol{\phi}$. Since the angle ϕ is so small, we can expand (43) in ascending powers of ϕ to find

$$\rho_\mathrm{f} = \rho_\mathrm{i} - \mathrm{i}\langle[\boldsymbol{\phi}\cdot\boldsymbol{S},\, \rho_\mathrm{i}]\rangle - \tfrac{1}{2}\langle\left[(\boldsymbol{\phi}\cdot\boldsymbol{S})^2\rho_\mathrm{i} + \rho_\mathrm{i}(\boldsymbol{\phi}\cdot\boldsymbol{S})^2 - 2\boldsymbol{\phi}\cdot\boldsymbol{S}\rho_\mathrm{i}\boldsymbol{\phi}\cdot\boldsymbol{S}\right]\rangle + \dots. \tag{44}$$

Let us assume that the rotation angle $\boldsymbol{\phi}$ is equally likely to point in any direction, so that if we average over all directions we find

$$\langle\boldsymbol{\phi}\rangle = 0 \tag{45}$$

and for products of the Cartesian components of $\boldsymbol{\phi}$, we find

$$\langle\phi_i\phi_j\rangle = \tfrac{1}{3}\delta_{ij}\langle\phi^2\rangle, \tag{46}$$

where $\langle\phi^2\rangle$ is the mean square rotation angle. Then (44) becomes

$$\rho_\mathrm{f} = \rho_\mathrm{i} - \frac{\langle\phi^2\rangle}{3}\left[S(S+1)\rho_\mathrm{i} - \boldsymbol{S}\cdot\rho_\mathrm{i}\boldsymbol{S}\right]. \tag{47}$$

EXERCISE 5

Derive (47) from (44).

If collisions occur at a rate $1/T$, then the density matrix evolves in time according to

$$\begin{aligned} \frac{\mathrm{d}\rho}{\mathrm{d}t} &= \frac{1}{T}(\rho_\mathrm{f} - \rho_\mathrm{i}) \\ &= -\frac{\langle\phi^2\rangle}{3T}\left[S(S+1)\rho_\mathrm{i} - \boldsymbol{S}\cdot\rho_\mathrm{i}\boldsymbol{S}\right]. \end{aligned} \tag{48}$$

Consider first the simple model discussed earlier of an alkali atom with no nuclear spin. Assume that the atomic spin polarization is purely longitudinal, i.e. it can be described by the probabilities $\rho(\pm 1/2)$ to find the electron spin pointing up or down, such that

$$\rho = \rho(1/2)\,|1/2\rangle\langle 1/2| + \rho(-1/2)\,|-1/2\rangle\langle -1/2| . \tag{49}$$

Equation (48) then becomes

$$\frac{\mathrm{d}\rho}{\mathrm{d}t} = -\frac{\langle\phi^2\rangle}{3T}\,\frac{3}{4}\rho + \frac{\langle\phi^2\rangle}{3T}\left(\frac{S_+\rho S_-}{2} + \frac{S_-\rho S_+}{2} + S_z\rho S_z\right). \tag{50}$$

Taking diagonal matrix elements of (50) we find

$$\begin{aligned}\frac{\mathrm{d}}{\mathrm{d}t}\rho(1/2) &= -\frac{\langle\phi^2\rangle}{4T}\rho(1/2) + \frac{\langle\phi^2\rangle}{6T}\rho(-1/2) + \frac{\langle\phi^2\rangle}{12T}\rho(1/2)\\ &= -\frac{\langle\phi^2\rangle}{6T}[\rho(1/2) - \rho(-1/2)]\end{aligned} \tag{51}$$

$$\frac{\mathrm{d}}{\mathrm{d}t}\rho(-1/2) = -\frac{\langle\phi^2\rangle}{6T}[\rho(-1/2) - \rho(1/2)] . \tag{52}$$

Using (51) and (52) we find the rate of change of the longitudinal spin polarization (4) to be

$$\begin{aligned}\frac{\mathrm{d}}{\mathrm{d}t}\langle S_z\rangle &= \frac{1}{2}\left[\frac{\mathrm{d}}{\mathrm{d}t}\rho(1/2) - \frac{\mathrm{d}}{\mathrm{d}t}\rho(-1/2)\right]\\ &= -\frac{\langle\phi^2\rangle}{6T}[\rho(1/2) - \rho(-1/2)]\\ &= -\frac{\langle\phi^2\rangle}{3T}\langle S_z\rangle .\end{aligned} \tag{53}$$

Thus, we see from (53) that in the absence of any optical pumping, the longitudinal electron spin polarization will relax with a single exponential having a time constant γ

$$\langle S_z\rangle = \langle S_z\rangle_0\,\mathrm{e}^{-\gamma t} . \tag{54}$$

where the electron spin randomization rate is related to the mean squared rotation angle $\langle\phi^2\rangle$ and the collision rate $1/T$ by

$$\gamma = \frac{\langle\phi^2\rangle}{3T} . \tag{55}$$

We can also correct the optical pumping equation (7) for the effects of spin relaxation and write the more realistic equation

$$\frac{\mathrm{d}}{\mathrm{d}t}\langle S_z\rangle = \frac{R}{3} - \left(\frac{2R}{3} + \gamma\right)\langle S_z\rangle . \tag{56}$$

If we solve (56) with the initial condition $\langle S_z \rangle = 0$ at $t = 0$, we find

$$\langle S_z \rangle = \frac{1}{2 + \frac{3\gamma}{R}} \left(1 - \mathrm{e}^{-(\gamma + 2R/3)t}\right). \tag{57}$$

The maximum attainable polarization

$$2\langle S_z \rangle = \frac{1}{1 + \frac{3\gamma}{2R}} \tag{58}$$

is now less than unity because of the effect of the spin relaxation. The polarization will be nearly total if $\gamma \ll R$, a situation which is easily realized in practice with an intense source of laser light and appropriately chosen buffer gases.

Some version of the simple model discussed above was often used to analyze the data of early optical pumping experiments, but it led to rather serious errors of interpretation. As experimental data began to accumulate, large discrepancies between the experimentally determined spin-relaxation cross sections of different laboratories were reported, and various attempts were made to account for the discrepancies. The major parts of this puzzle were solved by M.A. Bouchiat [11], who pointed out two important facts. First, the observed spin relaxation transients were not described by a single exponential decay curve, but in many cases the observed transient was the superposition of two or more exponential curves with time constants which could differ by more than an order of magnitude, as will be discussed in the following section. Some early experimenters had been measuring the longest time constants and some others had been measuring the shortest time constant. A second problem pointed out by Bouchiat was that the relaxation was often dominated by the formation of loosely bound Van der Waals molecules, consisting of an alkali atom attached to one of the heavier noble gas atoms, Ar, Kr, or Xe. The peculiar pressure dependence of the relaxation due to the Van der Waals molecules contributed to the misinterpretation of the experimental data.

10. Multiple time constants for the spin relaxation of alkali atoms

The existence of several different exponential time constants in the decay transients of alkali atoms is an effect of the nuclear spin. All stable alkali atoms have non-zero nuclear spins. Typical values of the nuclear spin quantum numbers are $I = 7/2$ for ^{133}Cs and $I = 3/2$ for ^{23}Na. We shall consider the relaxation of an alkali atom with the smallest possible non-zero nuclear spin, $I = 1/2$. Although no non-radioactive alkali atoms have such a small nuclear spin, the basic

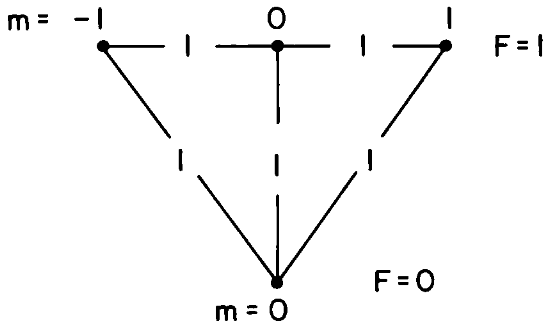

Fig. 7. Hyperfine energy levels of an atom with nuclear spin $I=1/2$ and the relative collisional relaxation rates between hyperfine energy levels in units of $\gamma/4$. The rate equations (71)–(74) can be written by inspection of this diagram.

physical causes of different relaxation time constants can be readily understood in this simple case, and the generalization of the results to higher nuclear spin quantum numbers is straightforward. The hyperfine structure of an alkali atom with $I=1/2$ is sketched in fig. 7, along with the collisional transfer rates between the sublevels. We shall discuss the transfer rates in more detail later.

The magnetic interaction between the valence electrons and the nuclear magnetic moment causes the energy levels to split into a triplet with total angular momentum $F=1$ and a singlet with $F=0$. The triplet will be further split into three azimuthal sublevels if a small magnetic field is present. As to order of magnitude, the hyperfine splitting of the ground state corresponds to a frequency in the GHz range, and the Zeeman splitting due to the magnetic field is 1.4 MHz/Gauss. One can think of the atom in fig. 7 as a hydrogen atom, although it is not easy to optically pump a hydrogen atom because the resonance lines are in the vacuum ultraviolet region of the spectrum, and the fine structure splitting of the 2^2 P state is very small.

We assume that the atomic polarization is well described by the sublevel populations, i.e. we can ignore any transverse spin polarization or off-diagonal elements of the density matrix. Then we can write

$$\rho=\sum|FmFm|\langle Fm|\rho(F,m). \tag{59}$$

The basic relaxation equation (48) remains valid for the atom with hyperfine structure, since we know that the duration of a binary collision is so short that we can ignore any modifications in the evolution of the atomic spins due to the hyperfine interaction during the short interval of a binary collision. However, the hyperfine coupling of the nucleus to the electron has an important effect in the relatively long intervals between collisions. Physically, we can imagine that the electron spin is rotated by a small angle during the binary collision, but that the corresponding rotation of the nuclear spin is negligible. Substituting (59) into (48) and taking diagonal matrix elements, we find that the rate equation for population transfer becomes

$$\begin{aligned}\frac{\mathrm{d}}{\mathrm{d}t}\rho(F,\, m) &= -\tfrac{3}{4}\gamma\rho(F,\, m) + \gamma\langle FM\,|\,\boldsymbol{S}\cdot\rho\boldsymbol{S}\,|\,Fm\rangle \\ &= -\sum_{F'm'} W(F,\, m;\; F',\, m')\rho(F',\, m'). \qquad (60)\end{aligned}$$

To evaluate the coupling coefficients W we note that

$$|11\rangle = \alpha(S)\alpha(I) \qquad (61)$$

$$10\rangle = \frac{1}{\sqrt{2}}\left[\alpha(S)\beta(I) + \beta(S)\alpha(I)\right] \qquad (62)$$

$$|1-1\rangle = \beta(S)\beta(I) \qquad (63)$$

$$|00\rangle = \frac{1}{\sqrt{2}}\left[\alpha(S)\beta(I) - \beta(S)\alpha(I)\right], \qquad (64)$$

where α and β denote spin-up and spin-down states of $I = 1/2$ and $S = 1/2$. Then, for example, one of the terms on the right of (60) becomes

$$\begin{aligned}\boldsymbol{S}\cdot|11\rangle\langle 11|\boldsymbol{S} &= \frac{S_{+}\,|11\rangle\langle 11|\,S_{-}}{2} + \frac{S_{-}\,|11\rangle\langle 11|\,S_{+}}{2} + S_z\,|11\rangle\langle 11|\,S_z \\ &= \tfrac{1}{4}\left[\,|11\rangle\langle 11| + |10\rangle\langle 10| + |00\rangle\langle 00| - |10\rangle\langle 00| - |00\rangle\langle 10|\,\right]. \qquad (65)\end{aligned}$$

We ignore off-diagonal terms like $|10\rangle\langle 00|$ since they oscillate rapidly at the hyperfine frequency and do not couple to the slowly changing diagonal terms. Thus we can conclude from (60) and (65) that

$$W(1,\, 1;\; 1,\, 1) = -\gamma/2 \qquad (66)$$

$$W(1,\, 0;\; 1,\, 1) = \gamma/4 \qquad (67)$$

$$W(0,\, 0;\; 1,\, 1) = \gamma/4 \qquad (68)$$

$$W(1,\, -1;\; 1,\, 1) = 0. \qquad (69)$$

The other columns of the rate matrix W can be evaluated in like manner. The elements in any column sum to zero, i.e.

$$\sum_{F,m} W(F,\, m;\; F',\, m') = 0. \qquad (70)$$

Formally, this condition guarantees that the relaxation process does not change the number of atoms in the sample.

EXERCISE 6

Show that (60) implies (70).

In view of (70) we can conveniently represent W in fig. 7 by labelling only the relative values of the non-zero, off-diagonal elements. We see that the collisional relaxation causes transitions at the same rate between all pairs of levels except (1, 1) and (1, −1). By inspection of fig. 7 we see that we can write out (60) as

$$\frac{\mathrm{d}}{\mathrm{d}t}\rho(1,1) = \tfrac{1}{4}\gamma[\rho(1,0) + \rho(0,0)] - \tfrac{1}{2}\gamma\rho(1,1) \tag{71}$$

$$\frac{\mathrm{d}}{\mathrm{d}t}\rho(1,0) = \tfrac{1}{4}\gamma[\rho(1,1) + \rho(0,0) + \rho(1,-1)] - \tfrac{3}{4}\gamma\rho(1,0) \tag{72}$$

$$\frac{\mathrm{d}}{\mathrm{d}t}\rho(1,-1) = \tfrac{1}{4}\gamma[\rho(1,0) + \rho(0,0)] - \tfrac{1}{2}\gamma\rho(1,-1) \tag{73}$$

$$\frac{\mathrm{d}}{\mathrm{d}t}\rho(0,0) = \tfrac{1}{4}\gamma[\rho(1,1) + \rho(1,0) + \rho(1,-1)] - \tfrac{3}{4}\gamma\rho(0,0). \tag{74}$$

We can simplify the rate equations above by taking certain linear combinations of populations which we write as follows:

$$\langle \boldsymbol{I}\cdot\boldsymbol{S}\rangle = \frac{\rho(1,1) + \rho(1,0) + \rho(1,-1)}{4} - \tfrac{3}{4}\rho(0,0) \tag{75}$$

$$\langle F_z\rangle = \rho(1,1) - \rho(1,-1) \tag{76}$$

$$\langle 3F_z^2 - \boldsymbol{F}\cdot\boldsymbol{F}\rangle = \rho(1,1) - 2\rho(1,0) + \rho(1,-1). \tag{77}$$

Then we note that

$$\frac{\mathrm{d}}{\mathrm{d}t}\langle \boldsymbol{I}\cdot\boldsymbol{S}\rangle = -\gamma\langle \boldsymbol{I}\cdot\boldsymbol{S}\rangle \tag{78}$$

$$\frac{\mathrm{d}}{\mathrm{d}t}\langle F_z\rangle = -\tfrac{1}{2}\gamma\langle F_z\rangle \tag{79}$$

$$\frac{\mathrm{d}}{\mathrm{d}t}\langle 3F_z^2 - \boldsymbol{F}\cdot\boldsymbol{F}\rangle = -\gamma\langle 3F_z^2 - \boldsymbol{F}\cdot\boldsymbol{F}\rangle. \tag{80}$$

Thus, the three observables (70)–(80) undergo simple exponential decay, but with two different rates. The hyperfine population imbalance (75) and the quadrupole polarization (77) both relax at the electron spin randomization rate γ. The longitudinal angular momentum (76) relaxes at half of the spin randomization rate, $\gamma/2$.

The analysis above shows that certain linear combinations of sublevel populations are especially convenient for the analysis of optical pumping and spin relaxation. The relaxation of these linear combinations is described by single exponential decay curves. We call these special linear combinations the *eigenobservables* of the system. One can always expand the density matrix as a superposition of eigenobservables P_i, i.e.

$$\rho = \frac{1}{G} + \sum_i f_i P_i, \tag{81}$$

where G, the statistical weight of the spin multiplet, is the number of spin sublevels, and the operators P_i are traceless and orthonormal, i.e.

$$\mathrm{Tr}\ P_i^\dagger P_j = \delta_{ij}. \tag{82}$$

The numbers f_i are the weights of each eigenobservable and are given by

$$f_i = \mathrm{Tr}\ P_i^\dagger \rho. \tag{83}$$

When the atoms are unpolarized all of the weights are zero and the atoms are equally likely to be found in any one of the spin sublevels.

EXERCISE 7
Derive (83).

In the example discussed above we found three eigenpolarizations for atoms which are undergoing electron spin randomizing collisions in a buffer gas. The normalized eigenobservables corresponding to (75)–(77) are:

$$P_0 = \sqrt{\tfrac{4}{3}}\,\boldsymbol{I}\cdot\boldsymbol{S} = \frac{1}{\sqrt{12}}\begin{pmatrix} 1 \\ 1 \\ 1 \\ -3 \end{pmatrix}, \tag{84}$$

where the elements of the column vector are the amplitudes of the basis operators $|11\rangle\langle 11|$, $|10\rangle\langle 10|$, $|1\ -1\rangle\langle 1\ -1|$ and $|00\rangle\langle 00|$ respectively. Similarly, we write a second eigenobservable

$$P_1 = \frac{F_z}{\sqrt{2}} = \frac{1}{\sqrt{2}}\begin{pmatrix} 1 \\ 0 \\ -1 \\ 0 \end{pmatrix} \tag{85}$$

and a third

$$P_2 = \frac{1}{\sqrt{6}}\left(3F_z^2 - \boldsymbol{F}\cdot\boldsymbol{F}\right) = \frac{1}{\sqrt{6}}\begin{pmatrix} 1 \\ -2 \\ 1 \\ 0 \end{pmatrix}. \tag{86}$$

Note that P_0, P_1 and P_2 are traceless, i.e., the sums of the 4 numbers in the

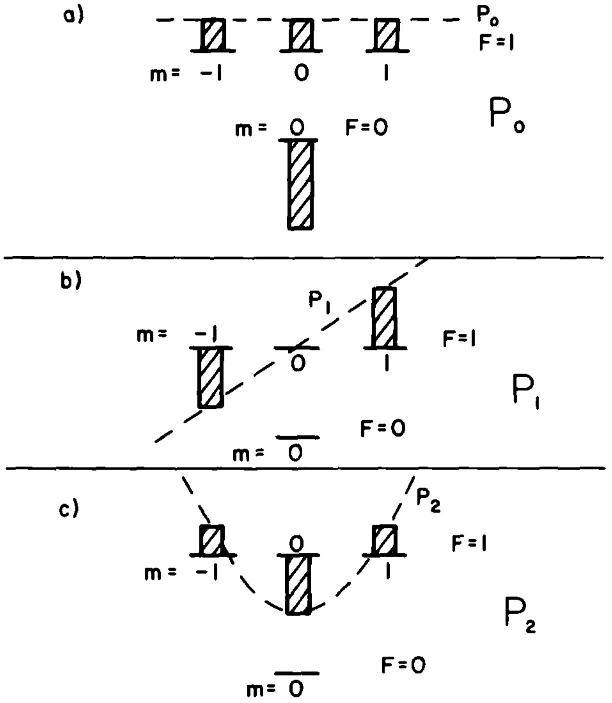

Fig. 8. Similarity between the dependence of $\langle m | P_l | m \rangle$ and the Legendre polynomial $P_l(m/J)$ on the azimuthal quantum number m.

columns are zero. We can completely describe the population imbalances of the H atom with these eigenpolarizations. The dependence of $\langle m | P_l | m \rangle$ on the azimuthal quantum number m is very similar to the dependence of the Legendre polynomials $P_l(m/J)$ as indicated in fig. 8. The similarity is not accidental and it is due to our assumption that the collisional relaxation mechanism responsible for the spin relaxation is isotropic.

Collisional transfer diagrams similar to fig. 7 can be sketched for $I > 1/2$. One finds that the collisional selection rules are $\Delta m = 0,\ \pm 1$, but the magnitudes of the rates are not all the same as is the case for the simple example of fig. 7. Bouchiat [11] has shown that $\boldsymbol{I} \cdot \boldsymbol{S}$ is always an eigenobservable which relaxes at the electron spin randomization rate. However there are two angular momentum eigenobservables [11], Q_e and $\bar{I}_z$ which, in the case of $I = 3/2$, have the population amplitudes sketched in fig. 9. $\bar{I}_z$ is defined to be

$$\bar{I}_z = \sum_{Fm} | Fm \rangle \langle Fm | I_z | Fm \rangle \langle Fm | . \tag{87}$$

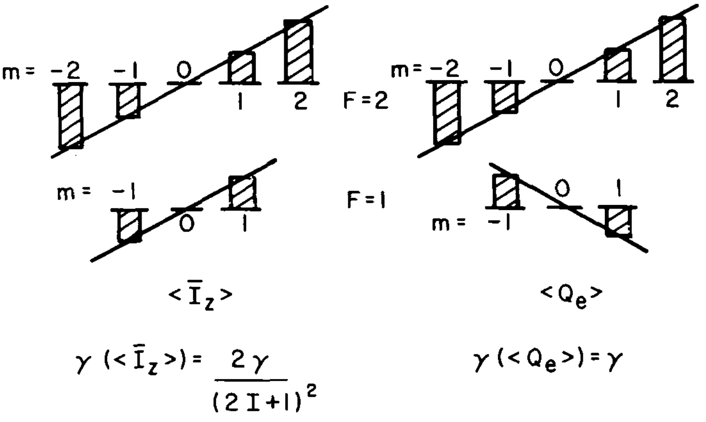

Fig. 9. The two angular momentum eigenobservables $\bar{I}_z$ and Q_e for an alkali atom with nuclear spin $I = 3/2$. The amplitudes can be calculated from (87) and (88) with the aid of the projection theorem for coupled angular momenta. The selection rules for the transitions caused by electron randomizing collisions are $\Delta F = 0, \pm 1$ and $\Delta m = 0, \pm 1$, i.e. transitions occur only between nearest neighbor sublevels. Thus Q_e relaxes faster than $\bar{I}_z$, since the nearest neighbor sublevels with $\Delta F = 1$ of the eigenobservable Q_e have larger population differences than do those of $\bar{I}_z$.

That is, $\bar{I}_z$ is the diagonal part of the longitudinal nuclear spin operator I_z. The other observable is

$$Q_e = \bar{S}_z - \frac{2}{2I+1}\bar{I}_z, \tag{88}$$

where $\bar{S}_z$ is defined in analogy to (87).

In many optical pumping experiments which use circularly polarized light, the signal is proportional to $\langle \bar{S}_z \rangle$, which is given by

$$\langle \bar{S}_z \rangle = \langle Q_e \rangle + \frac{2}{2I+1}\langle \bar{I}_z \rangle. \tag{89}$$

It can be shown [11] that the relaxation transients will decay with two different exponential time constants, a fast decay at the electron spin randomization rate γ, the decay rate of $\langle Q_e \rangle$, and a slow decay of $\langle \bar{I}_z \rangle$ at the rate $2\gamma(2I+1)^{-2}$ or $\gamma/8$ as is illustrated in fig. 9. For quantitative measurements of relaxation phenomena it is important to be aware of the possibility that the relaxation transients may be superpositions of exponentials with quite different time constants.

11. Van der Waals molecules

An important relaxation mechanism which was not understood in early optical pumping experiments and which led to considerable confusion until it was

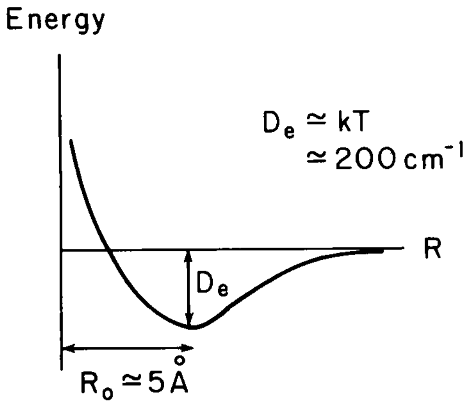

Fig. 10. Interaction potential between an alkali and a noble gas atom for a Van der Waals molecule. At a representative internuclear separation of 5 Å, the well depth might be 200 cm^{-1}.

recognized by Bouchiat and her coworkers [11] is the formation of loosely bound Van der Waals molecules. There is a weak attractive well in the interaction potential between an alkali atom and a noble gas atom as sketched in fig. 10. The well depth is only on the order of kT at room temperature, so the molecules can be broken up by almost any collision. However, the molecule is perfectly stable in the intervals between collisions. The intervals between collisions can be hundreds of nanoseconds at buffer gas pressures of a few Torr, and as short as one nanosecond at buffer gas pressures on the order of one atmosphere. These time intervals are much longer than the picosecond duration of a binary collision, so the spin flip probabilities of an alkali atom in a Van der Waals molecule can approach unity since the flipping probability scales as the square of the interaction time. In fact, the existence of long-lived Van der Waals molecules would cause such rapid relaxation that it would be impossible to produce high spin polarization if it were not for the fact that an improbable three-body collision is required for a Van der Waals molecule to form. A typical formation event is illustrated in fig. 11. The nitrogen molecule or another Xe or Rb atom is needed as a third body to carry away the binding energy of the molecule.

For the simple model of an alkali atom with no nuclear spin, the relaxation caused by Van der Waals molecules can be described by the rate equation

$$\frac{d\rho}{dt} = \frac{1}{T_F}(\rho_f - \rho_i), \tag{90}$$

where the three-body formation rate per alkali atom is

$$\frac{1}{T_F} = [Xe][N_2]Z. \tag{91}$$

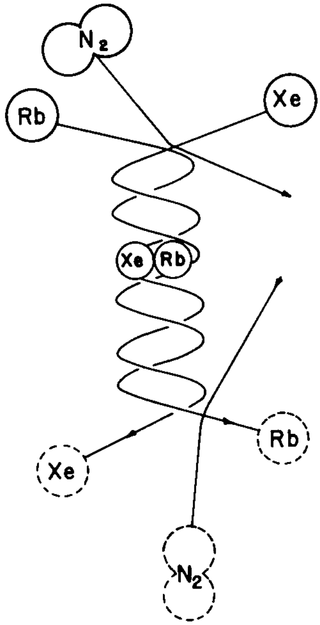

Fig. 11. Formation of a Van der Waals molecule. Van der Waals molecules such as RbXe, are formed in a 3 body collision. The third body eg. N_2, is required to simultaneously satisfy conservation of energy and momentum.

Here Z is a characteristic rate constant which is typically on the order of 10^{-34} cm^6 sec^{-1}. The final density operator is described by (43) which we can no longer approximate with the power series expansion (44) because the rotation angle ϕ can be many radians in a long-lived Van der Waals molecule. Let us consider

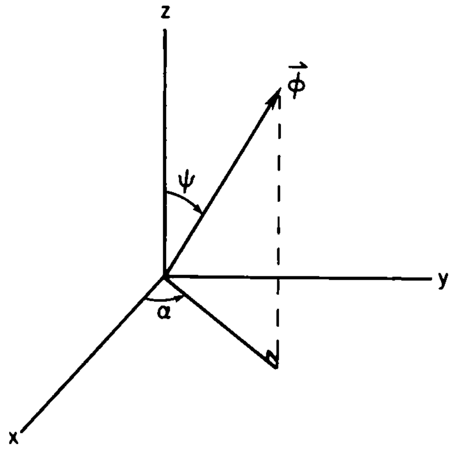

Fig. 12. Coordinate system used to represent ϕ.

again the simple model of an alkali atom with no nuclear spin which is described by the density operator (23). Then the final density operator after the collision is

$$\rho_{\mathrm{f}} = \left\{ \mathrm{e}^{-\mathrm{i}\boldsymbol{\phi}\cdot\boldsymbol{S}} \left[\tfrac{1}{2} + 2\langle S_z\rangle S_z \right] \mathrm{e}^{\mathrm{i}\boldsymbol{\phi}\cdot\boldsymbol{S}} \right\}_{\phi}$$
$$= \tfrac{1}{2} + 2\langle S_z\rangle \left\{ \mathrm{e}^{-\mathrm{i}\boldsymbol{\phi}\cdot\boldsymbol{S}} S_z \, \mathrm{e}^{\mathrm{i}\boldsymbol{\phi}\cdot\boldsymbol{S}} \right\}_{\phi}. \tag{92}$$

The notation $\{\ \ \}_{\phi}$ denotes an average over the direction and magnitude of $\boldsymbol{\phi}$. The coordinate system used to represent $\boldsymbol{\phi}$ is shown in fig. 12. If we average over the azimuthal angle α we find

$$\left\{ \mathrm{e}^{-\mathrm{i}\boldsymbol{\phi}\cdot\boldsymbol{S}} S_z \, \mathrm{e}^{\mathrm{i}\boldsymbol{\phi}\cdot\boldsymbol{S}} \right\}_{\phi} = S_z \left[\cos^2\psi + \sin^2\psi \cos\phi \right]. \tag{93}$$

Next, (93) is averaged over an isotropic distribution of ψ such that $\langle\cos^2\psi\rangle = 1/2$ and $\langle\sin^2\psi\rangle = 2/3$ yielding

$$\left\{ \mathrm{e}^{-\mathrm{i}\boldsymbol{\phi}\cdot\boldsymbol{S}} S_z \, \mathrm{e}^{\mathrm{i}\boldsymbol{\phi}\cdot\boldsymbol{S}} \right\}_{\phi} = \tfrac{1}{3} S_z [1 + 2 \mathit{cos}\, \phi]. \tag{94}$$

EXERCISE 8
Verify (94).

Finally, if we assume an exponential probability distribution of rotation angles, corresponding to an exponential distribution of molecular lifetimes

$$P(\phi)\,\mathrm{d}\phi = \exp(-\phi/\bar{\phi}) \frac{\mathrm{d}\phi}{\bar{\phi}}, \tag{96}$$

we find the average value of (96) to be

$$\left\{ \mathrm{e}^{-\mathrm{i}\boldsymbol{\phi}\cdot\boldsymbol{S}} S_z \, \mathrm{e}^{\mathrm{i}\boldsymbol{\phi}\cdot\boldsymbol{S}} \right\}_{\phi} = \frac{S_z}{3} \left[1 + \frac{2}{1 + \bar{\phi}^2} \right] \tag{97}$$

and hence from (97) and (90)

$$\rho_{\mathrm{f}} = \frac{1}{2} + \frac{2}{3} \left[1 + \frac{2}{1 + \bar{\phi}^2} \right] \langle S_z\rangle S_z. \tag{98}$$

Then the evolution equation becomes

$$\frac{\mathrm{d}}{\mathrm{d}t}\langle S_z\rangle = -\frac{2}{3T_{\mathrm{F}}} \frac{\bar{\phi}^2}{1 + \bar{\phi}^2} \langle S_z\rangle = -\gamma\langle S_z\rangle. \tag{99}$$

Note that $\langle\phi^2\rangle$ of (46) is the same as $2\bar{\phi}^2$. The rotation angle is inversely proportional to the third body pressure so we can write

$$\bar{\phi} = \frac{p_0}{p}, \tag{100}$$

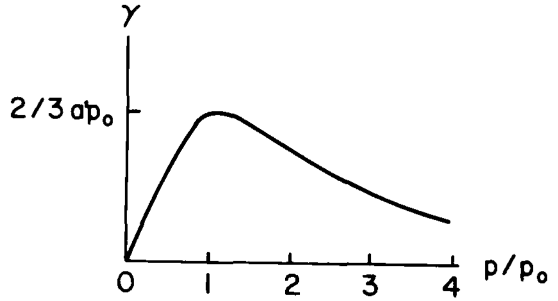

Fig. 13. Dependence of the spin depolarization rate γ on the third body pressure p. Here we assume that the spin polarized atom sticks to a heavy noble gas atom whose partial pressure is negligible compared to that of a "third body gas" like N_2 or He which does not form Van der Waals molecules or cause noticeable spin relaxation.

where p_0 is some characteristic pressure, typically about 100 Torr, at which the mean rotation angle is 1 radian. Also, the three body formation rate is proportional to the product of the noble gas pressure and the third body pressure p. We assume that the cell contains a small fixed amount of a heavy noble gas like Xe which can form Van der Waals molecules with the alkali atom and a much larger pressure p of some gas like Ni_2 which does not readily form Van der Waals molecules and which causes negligible spin relaxation but which can act as a third body in the formation of the molecule. Then the formation rate will be

$$\frac{1}{T_F} = ap, \tag{101}$$

where a is some constant. The spin depolarization rate should then scale as

$$\gamma = \tfrac{2}{3} a p_0^2 \frac{p}{p^2 + p_0^2}. \tag{102}$$

The expected pressure dependence of γ is shown in fig. 13. The peculiar pressure dependence sketched above is characteristic of a situation where the spin-polarized alkali atoms are relaxing in a small fixed amount of a heavy noble gas (for example 1 Torr of Xe) in the presence of a much larger amount of a third-body gas of pressure p.

If the alkali vapor is relaxing in pure Xe or Kr gas, then the Xe or Kr atom must also serve as the third body and the molecular formation rate is proportional to the square of the gas pressure, i.e.

$$\frac{1}{T_F} = bp^2, \tag{103}$$

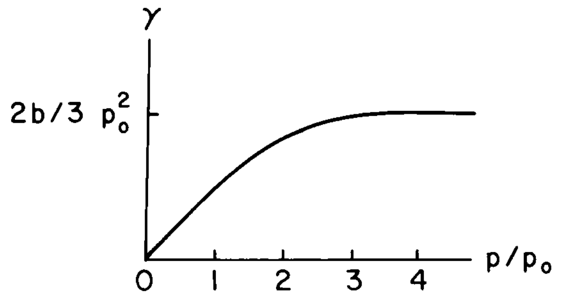

Fig. 14. Dependence of the spin depolarization rate γ on the noble gas pressure p. Here we assume that the heavy noble gas also serves as a third body.

where b is some constant. Substituting (103) into (99) we find that the relaxation rate is

$$\gamma = \tfrac{2}{3} b p_0^2 \frac{p^2}{p_0^2 + p^2}\,. \tag{104}$$

The expected pressure dependence of γ as a function of the pure noble gas pressure is shown in fig. 14.

12. Relaxation due to spatial diffusion

Spin polarized atoms can diffuse through the buffer gas of a sample cell to the cell walls. It is often true that the cell walls are an effective mechanism for spin depolarization. If we ignore the effects of spin depolarization due to collisions with the buffer gas, the atomic density operator will obey the diffusion equation

$$\frac{\mathrm{d}\rho}{\mathrm{d}t} = D\nabla^2\rho, \tag{105}$$

where

$$D = \lambda v/3 \tag{106}$$

is the diffusion constant of the atoms in the gas, λ is the mean free path of diffusing atoms in the gas and v is the mean thermal velocity. To solve the diffusion equation we need to know the boundary conditions at the cell walls. When an atom strikes the cell wall it may stick for some dwell time. While the atom is on the wall various spin relaxation processes will be at work. For example, there may be paramagnetic sites on the cell wall like dangling chemical bonds which interact with the electron spin of the atom or with the nuclear magnetic dipole moment. There will also be large electric field gradients which can interact with the nuclear quadrupole moments of diamagnetic atoms like ^{131}Xe. Let us suppose that the wall destroys a fraction α_i of the eigenobservable amplitude f_i, but that the wall causes no mixing of the eigenobservable amplitudes with each other. Then the gas kinetic current j_{i+} of the eigenobservable amplitude f_i into the wall is

$$j_{i+} = N\left[\frac{vf_i}{4} - \frac{D}{2}\frac{\partial}{\partial n}f_i\right], \tag{107}$$

where N is the total number density of spin polarized atoms and

$$\frac{\partial}{\partial n} = \boldsymbol{n}\cdot\nabla$$

is the spatial gradient along a unit vector $\boldsymbol{n}$, normal to the wall and pointing out of the cell. All of the adsorbed atoms eventually desorb from the wall and they carry with them a fraction $(1-\alpha_i)$ of the polarization amplitude f_i. Thus, we can write for the desorbing current

$$j_{i-} = (1-\alpha_i)\,j_{i+}. \tag{108}$$

Let us assume that the total current into the wall obeys the usual formula for diffusional transport

$$j_{i+} - j_{i-} = ND\frac{\partial f_i}{\partial t}. \tag{109}$$

Substituting (105) and (109) into (107) we find that the boundary condition at the wall must be

$$\frac{\partial f_i}{\partial n} = -\mu_i f_i, \tag{110}$$

where the normal gradient parameter is

$$\mu_i = \frac{3\alpha_i}{2(2-\alpha_i)\lambda}. \tag{111}$$

Strictly speaking, one should think of μ_i as a function of position on the cell surface. It can be a complex number if there are coherent wall interactions, and it can be an operator if the wall interactions are coherent and mix different eigenobservables. For simplicity we shall regard μ_i as a real constant. If we consider the evolution of spin-polarized atoms under the simultaneous influence of diffusion and spin relaxation in the bulk, we find that in the gas the amplitude of an eigenobservable satisfies the equation

$$\frac{\mathrm{d}f_i}{\mathrm{d}t} = D\nabla^2 f_i - \gamma_i f_i. \tag{112}$$

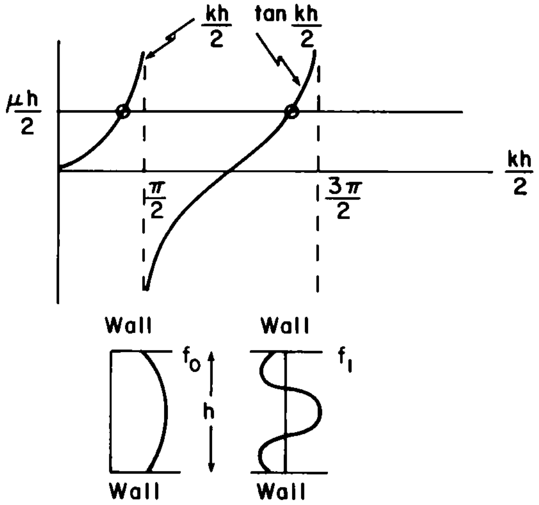

Fig. 15. Graphical solution of equation (117). Two possible solutions for the spatial frequency k and the corresponding spatial diffusion modes are sketched for the case where polarized atoms are confined between two infinite plane parallel walls separated by a distance h.

Let us seek an exponentially decaying solution to (112) of the form

$$f_i = f_i(\boldsymbol{r})\,\mathrm{e}^{-\Gamma t}. \tag{113}$$

Then (112) becomes the purely spatial equation

$$[\nabla^2 + k^2] f_i = 0, \tag{114}$$

where the spatial frequency k is related to the other parameters by

$$\Gamma = \gamma_i + Dk^2. \tag{115}$$

The solution to (114) subject to the boundary condition (110) can be quite involved for complicated cell shapes, but one can get a good physical insight into the issues involved by considering atoms which are confined between two infinite plane parallel walls located at $z = \pm h/2$. Then a symmetric solution to (114) is

$$f_i = A \cos kz \tag{116}$$

which satisfies the boundary condition (110) if

$$k \tan(kh/2) = \mu. \tag{117}$$

This transcendental equation can be solved graphically as indicated in fig. 15. The solutions are indicated by circles, and their spatial dependences are sketched below.

For the most slowly relaxing mode we can consider two limiting cases. We first consider a "good", weakly relaxing wall for which

$$\mu h/2 \ll 1. \tag{118}$$

We assume that (117) implies also that

$$kh2 \ll 1 \tag{119}$$

so we can set tan $kh/2 \approx kh/2$ in (117) and write

$$k^2 = 2\mu/h. \tag{120}$$

There must also be a very small spin destruction probability at the wall to ensure the validity of (118) so we can approximate (111) by

$$\mu \approx 3\alpha/4\lambda. \tag{121}$$

Then the spin relaxation rate Γ becomes

$$\Gamma = \gamma_i + \frac{v\alpha_i}{2h}. \tag{122}$$

That is, for a good wall, the wall contribution to the relaxation rate (122) is independent of the gas pressure. Increasing the gas pressure for a cell with good walls causes the spins to relax faster, since it will increase the bulk relaxation rate γ_i while having no effect on the wall rate. This is the situation which can be realized for alkali atoms in glass cells with paraffin-coated walls at low buffer gas pressures or for mercury or noble gas atoms with nuclear spin polarization in uncoated glass or quartz cells.

A second important limiting case is that of a very strongly depolarizing cell wall for which $\alpha_i \approx 1$ and

$$\mu h/2 \gg 1. \tag{123}$$

Then we see from fig. 15 that for the slowest diffusion mode

$$kh/2 \approx \pi/2, \tag{124}$$

so the relaxation rate (115) becomes

$$\Gamma = \gamma_i + D(\pi/h)^2. \tag{125}$$

Under these conditions the contribution of the wall to the relaxation rate is proportional to the diffusion constant D and it is therefore inversely proportional to the buffer gas pressure. This is the sort of situation which is realized for spin polarized alkali atoms in uncoated glass cells where the walls are very strongly depolarizing. Every atom which diffuses to the cell walls will lose its spin before desorbing from the wall. For such cells high pressures of weakly relaxing buffer gases are favorable since they slow down the diffusion of the polarized atoms to the walls.

13. Relaxation due to spin exchange

As a final topic we shall discuss the important phenomenon of spin exchange which makes it possible to transfer spin polarization from atoms which can be easily optically pumped, especially the alkali atoms, to atoms which are difficult to spin polarize by direct optical pumping. Some examples of atoms which are very conveniently polarized by spin exchange are hydrogen atoms, nitrogen atoms and the nuclear spins of noble gas atoms. None of these atoms can be easily optically pumped directly because their resonance absorption lines lie in the vacuum ultraviolet region of the spectrum where there are no good sources of pumping radiation and where optical components like lenses and mirrors are expensive or unobtainable. Here we shall consider spin exchange between electron spins, but entirely analogous considerations hold for spin exchange between polarized electrons and nuclei. We may write the spin exchange process between an alkali atom A and a hydrogen atom H symbolically as

$$\mathrm{A}(\uparrow) + \mathrm{H}(\downarrow) \rightarrow \mathrm{A}(\downarrow) + \mathrm{H}(\uparrow). \tag{126}$$

The origin of the spin exchange interaction is the splitting of the singlet and triplet potential curves of the HA molecule which is sketched in fig. 16 as a function of the internuclear separation *R*. Just before the spin exchange collision, we can write the wave function of the HA pair as

$$|\psi_i\rangle = \psi_A\rangle\,|\psi_H\rangle. \tag{127}$$

This wavefunction will contain electronic-spin singlet and triplet components,

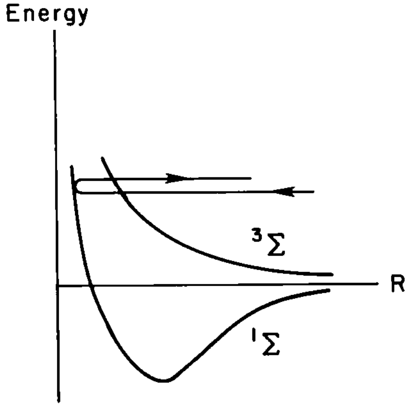

Fig. 16. Splitting of the singlet and triplet potential curves of the HA molecule. The classical trajectory of a particle scattering from the $^1\Sigma$ potential is also shown.

which we can project out of the wavefunction by means of the projection operators

$$P_s = \tfrac{1}{4} - \boldsymbol{S}_A \cdot \boldsymbol{S}_B$$

$$P_t = \tfrac{3}{4} + \boldsymbol{S}_A \cdot \boldsymbol{S}_B . \qquad (128)$$

EXERCISE 9

Derive P_s and P_t.

The final wavefunction after the collision will be

$$|\psi_f\rangle = U|\psi_i\rangle , \qquad (129)$$

where the unitary operator U is

$$U = e^{-i\phi_s} P_s + e^{-i\phi_t} P_t \qquad (130)$$

and the phase evolution angles can be writen in the semiclassical approximation in terms of the integral of the potential curves along the classical trajectories

$$\phi_s = \int_{-\infty}^{\infty} \frac{V_s}{\hbar} \mathrm{d}t \qquad (131)$$

$$\phi_t = \int_{-\infty}^{\infty} \frac{V_t}{\hbar} \mathrm{d}h . \qquad (132)$$

If we work with density operators, (130) implies that

$$(\rho_{HA})_f = U(\rho_{HA})_i U^{\dagger} , \qquad (133)$$

where for uncorrelated ensembles of atoms A and H the density operator of a colliding pair is simply

$$(\rho_{HA})_i = \rho_A \rho_H . \qquad (134)$$

Substituting (130) into (133) we find

$$(\rho_{HA})_f = P_s \rho_H \rho_A P_s + P_t \rho_H \rho_A P_t + \left(P_s \rho_H \rho_A P_t \, e^{i\Delta\phi} + \text{h.c.} \right) , \qquad (135)$$

where h.c. denotes the Hermitian conjugate of the previous expression, and the phase difference is

$$\Delta\phi = \phi_t - \phi_s . \qquad (136)$$

Substituting (128) and (134) into (135) and carrying out the algebra we find

$$(\rho_{HA})_f = \rho_A \rho_H + \sin^2 \frac{\Delta\phi}{2} \left[-\tfrac{3}{4} \rho_A \rho_H + \boldsymbol{S}_A \cdot \boldsymbol{S}_H \rho_A \rho_H + \rho_A \rho_H \boldsymbol{S}_A \cdot \boldsymbol{S}_H \right.$$

$$\left. + 4 \boldsymbol{S}_A \cdot \boldsymbol{S}_H \rho_A \rho_H \boldsymbol{S}_A \cdot \boldsymbol{S}_H \right] + i \sin \Delta\phi [\boldsymbol{S}_A \cdot \boldsymbol{S}_H , \rho_A \rho_H] . \qquad (137)$$

EXERCISE 10

Verify (137). Hint: for a spin-1/2 particle note that the spin operators satisfy the identities $S_iS_j + S_jS_i = \delta_{ij}/2$ where $i,\ j = x,\ y,\ z$.

We assume that the density operators of the A atoms and the H atoms remain uncorrelated after the spin exchange collisions because of the random nature of collisions in a gas cell. Then we can write

$$\frac{\mathrm{d}}{\mathrm{d}t}(\rho_{\mathrm{H}})_{\mathrm{ex}} = \frac{1}{T}\left[\mathrm{Tr}_{\mathrm{A}}(\rho_{\mathrm{HA}})_{\mathrm{f}} - \rho_{\mathrm{H}}\right], \tag{138}$$

where $1/T$ is the collision rate. Substituting (137) into (138) we find

$$\begin{aligned}\frac{\mathrm{d}}{\mathrm{d}t}(\rho_{\mathrm{H}})_{\mathrm{ex}} = \frac{1}{T_{\mathrm{ex}}}\big[&-\tfrac{3}{4}\rho_{\mathrm{H}} + \boldsymbol{S}_{\mathrm{H}}\cdot\rho_{\mathrm{H}}\boldsymbol{S}_{\mathrm{H}} + \langle \boldsymbol{S}_{\mathrm{A}}\rangle\cdot\boldsymbol{S}_{\mathrm{H}}\rho_{\mathrm{H}} + \rho_{\mathrm{H}}\boldsymbol{S}_{\mathrm{H}}\cdot\langle \boldsymbol{S}_{\mathrm{A}}\rangle \\ &- 2\mathrm{i}\langle \boldsymbol{S}_{\mathrm{A}}\rangle\cdot(\boldsymbol{S}_{\mathrm{H}}\times\rho_{\mathrm{H}}\boldsymbol{S}_{\mathrm{H}})\big] - \mathrm{i}[\delta\boldsymbol{\omega}\cdot\boldsymbol{S}_{\mathrm{H}},\ \rho_{\mathrm{H}}],\end{aligned} \tag{139}$$

where the spin exchange rate is

$$\frac{1}{T_{\mathrm{ex}}} = \frac{1}{T}\left\langle \sin^2\frac{\Delta\phi}{2}\right\rangle \tag{140}$$

and the rotation rate is

$$\delta\boldsymbol{\omega} = \frac{\langle \sin\,\Delta\phi\rangle}{T}\langle \boldsymbol{S}_{\mathrm{A}}\rangle. \tag{141}$$

EXERCISE 11

Verify (139).

We note that if the atoms A are unpolarized so that $\langle \boldsymbol{S}_{\mathrm{A}}\rangle = 0$, the spin exchange equation (139) becomes identical to the equation for electron spin randomization (50) where we must identify $\langle\phi^2\rangle/3T$ with $1/T_{\mathrm{ex}}$. It is not difficult to show that (139) implies that

$$\begin{aligned}\frac{\mathrm{d}\langle \boldsymbol{S}_{\mathrm{H}}\rangle}{\mathrm{d}t} &= \mathrm{Tr}\left(\boldsymbol{S}_{\mathrm{H}}\frac{\mathrm{d}\rho_{\mathrm{H}}}{\mathrm{d}t}\right) \\ &= \frac{1}{T_{\mathrm{ex}}}[\langle \boldsymbol{S}_{\mathrm{A}}\rangle - \langle \boldsymbol{S}_{\mathrm{H}}\rangle].\end{aligned} \tag{142}$$

EXERCISE 12

Verify (142).

That is, in equilibrium we must have

$$\langle \boldsymbol{S}_{\mathrm{H}}\rangle = \langle \boldsymbol{S}_{\mathrm{A}}\rangle. \tag{143}$$

Thus, if there is no nuclear spin the equilibrium density operator of the H atoms is

$$\rho_H = \tfrac{1}{2} + 2\langle \boldsymbol{S}_A \rangle \cdot \boldsymbol{S}_H. \tag{144}$$

If the atom H has a non-zero nuclear spin I, a solution to (139) for which $d\rho_H/dt = 0$ is

$$\rho_H = (\tfrac{1}{2} + 2\langle \boldsymbol{S}_A \rangle \cdot \boldsymbol{S}_H)\rho_I, \tag{145}$$

where ρ_I is any normalized density operator which operates only on the nuclear spin variables.

However, in general (145) is not a steady state solution for the spin polarized atoms because the true evolution equation for the spin polarized atoms is not (139) but

$$\frac{d\rho_H}{dt} = \frac{d}{dt}(\rho_H)_{ex} + \frac{1}{i\hbar}[A\boldsymbol{I}\cdot\boldsymbol{S}, \rho_H]. \tag{146}$$

That is, we must account for the hyperfine coupling of the electron spin $\boldsymbol{S}$ and the nuclear spin $\boldsymbol{I}$ by the magnetic dipole hyperfine interaction $A\boldsymbol{I}\cdot\boldsymbol{S}$. There is only one possible equilibrium solution to (146), as was first pointed out by Anderson et al. [12]. The solution is

$$\rho_H = N\,e^{\boldsymbol{\beta}\cdot\boldsymbol{F}}, \tag{147}$$

where N is a constant which can be determined from the requirement that $\mathrm{Tr}[\rho] = 1$. The total angular momentum of the H atom is

$$\boldsymbol{F} = \boldsymbol{S} + \boldsymbol{I} \tag{148}$$

and the constant vector $\boldsymbol{\beta}$, *the spin temperature parameter*, is defined by

$$\boldsymbol{\beta} = [2\tanh^{-1} 2|\langle \boldsymbol{S}_A \rangle|]\frac{\langle \boldsymbol{S}_A \rangle}{|\langle \boldsymbol{S}_A \rangle|}. \tag{149}$$

EXERCISE 13

Verify (149). *Hint*: $[\boldsymbol{F}, \boldsymbol{I}\cdot\boldsymbol{S}] = 0$

The spin temperature distribution $\rho = e^{\beta F_z}$ is sketched in Fig. 17. Note that the spin temperature distribution is a complicated superposition of the eigenpolarizations we discussed in connection with electron spin randomization in Section 10. For sufficiently dense alkali vapors the very important spin temperature distribution (147) is a good description of the spin polarization.

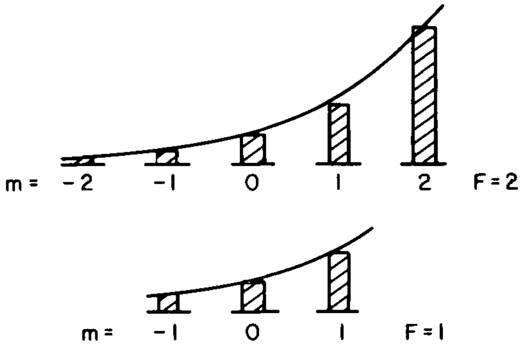

Fig. 17. Spin temperature distribution. It is possible to define an effective temperature $kT = \beta^{-1}$, which can be used to determine the sublevel occupation probability for alkali atoms which are having rapid spin exchange collisions with each other.

References

[1] Rev. Mod. Phys. 44 (1972) 169.
[2] A.J. Kastler, Phys. Radium 11 (1950) 225.
[3] J. Brossel and F. Bitter, Phys. Rev. 86 (1952) 308.
[4] P.A. Franken, Phys. Rev. 121 (1961) 1508.
[5] G.E. Pake, *Frontiers In Physics: Paramagnetic Resonance* (W.A. Benjamin, Inc. New York, 1962).
[6] F.A. Franz, Phys. Rev. 141 (1966) 105.
[7] W. Happer, K.D. Bonin and T.G. Walker, Phys. Lett. A 120 (1987) 105.
[8] R.A. Bernheim, J. Chem. Phys. 36 (1962) 135.
[9] R.H. Herman, Phys. Rev. 136 (1964) A1576.
[10] Z. Wu et al., Phys. Rev. Lett. 54 (1985) 1921.
[11] M.A. Bouchiat et al, J. Chem. Phys. 56 (1972) 3703.
[12] L.W. Anderson et al., Phys. Rev. 120 (1960) 1279.